Biogeochemistry (2009) 94:13–28
DOI 10.1007/s10533-009-9296-x

# Bioavailability of organic matter in a freshwater estuarine sediment: long-term degradation experiments with and without nitrate supply

**Jeffrey Abell · Anniet M. Laverman · Philippe Van Cappellen**

Received: 7 August 2008 / Accepted: 11 February 2009 / Published online: 26 March 2009


**Abstract** Organic carbon degradation experiments were carried out using flow-through reactors with sediments collected from an intertidal freshwater marsh of an eutrophic estuary (The Scheldt, Belgium). Concentrations of nitrate, nitrite, dissolved inorganic carbon (DIC), dissolved organic carbon, methane, dissolved cations ($Ca^{2+}$, $Mg^{2+}$, $Na^{+}$ and $K^{+}$), total dissolved Fe, phosphate and alkalinity were measured in the outflow solutions from reactors that were supplied with or without the terminal electron acceptor nitrate. Organic carbon mineralization rates were computed from the release rates of DIC after correcting for the contribution of carbonate mineral dissolution. The experiments ran for several months until nitrate reducing activity could no longer be detected. In the reactors supplied with nitrate, 10–13% of the bulk sedimentary organic carbon (SOC) was mineralized by the end of the experiments. In reactors receiving no nitrate, only 3–9% of the initial SOC was mineralized. Organic matter utilization by nitrate reducers could be described as the simultaneous degradation of two carbon pools with different maximum oxidation rates and half-saturation constants. Even when nitrate was supplied in non-limiting concentrations about half of the carbon mineralization in the reactors was due to fermentative processes, rather than being coupled to nitrate respiration. Fermentation may thus be responsible for a large fraction of the DIC efflux from organic-rich, nearshore sediments.

**Keywords** Organic carbon · Sediment · Bioavailability · Degradation · Nitrate reduction · Denitrification · Fermentation · Scheldt estuary

J. Abell · A. M. Laverman · P. Van Cappellen
Department of Earth Sciences – Geochemistry, Faculty of Geosciences, Utrecht University, P.O. Box 80021, 3508TA Utrecht, The Netherlands

*Present Address:*
J. Abell
Department of Oceanography, Humboldt State University, 1 Harpst Street, Arcata, CA 95521, USA
e-mail: ja49@humboldt.edu

A. M. Laverman (✉)
UMR 7619 Sisyphe, Université Pierre et Marie Curie, 4 Place Jussieu, 75005 Paris Cedex 05, France
e-mail: Anniet.Laverman@upmc.fr

P. Van Cappellen
School of Earth and Atmospheric Sciences, Georgia Institute of Technology, Atlanta, GA 30332-0340, USA
e-mail: pvc@eas.gatech.edu

## Introduction

The reactivity and availability of organic matter strongly affect the biogeochemistry, redox structure and geomicrobiology of aquatic sediments (Van

Cappellen and Gaillard 1996; Beauchamp et al. 1989). Yet, there exists little quantitative information on the in situ bioavailability of sedimentary organic matter, or on how organic matter availability relates to microbial degradation pathways and rates (Arnosti and Holmer 2003; Arnosti 2004). To a large degree this is due to the complex physicochemical nature of sedimentary organic matter, comprising pools of variable accessibility and degradability, but it may also be due to intrinsic differences between biochemical degradation pathways which are not yet completely understood (Arnosti 2004).

In order to be oxidized, sedimentary organic matter must first be broken down into monomeric organic compounds, via a combination of extracellular hydrolysis and fermentation (Fenchel and Findlay 1995; Mayer 1989). The limited number of published studies suggests that the initial production of these smaller organic substrates controls the net rate of organic carbon oxidation (Hoppe 1991; Lehman and O'Connell 2002). This is the starting assumption for most early diagenetic models describing organic matter degradation (Van Cappellen and Gaillard 1996). There is mounting evidence, however, that the nature of the terminal electron acceptor also affects the kinetics of organic matter degradation (e.g., Pallud et al. 2007).

Several recent studies have used flow-through reactors containing intact sediment slices to determine the kinetics for various microbial respiration pathways: namely nitrate reduction, sulfate reduction and the coupling of hydrolytic activity to terminal metabolism (Laverman et al. 2006; Pallud and Van Cappellen 2006; Roychoudhury et al. 2003; Bruchert and Arnosti 2003). These reactors have the advantage that rates can be measured under a wide range of experimental conditions with minimal disturbance to the physical and microbial structure of the sediment (Pallud et al. 2007). So far, these studies have focused on the dependence of microbial respiration rates on the availability of the terminal electron acceptor, at time scales over which changes in the abundance and reactivity of the organic electron donors are sufficiently small to allow the reacting system to approach steady state conditions.

Here, long-term flow-through reactors are used to quantify the fraction of sedimentary organic matter that is bioavailable when an external electron acceptor (nitrate) is supplied at non-limiting concentrations and when no terminal electron acceptor is provided. A tandem flow-through reactor approach is used to determine the relative importance of respiration and fermentation in the mineralization of sedimentary organic matter, and to assess the role of available sedimentary organic carbon in the kinetics of nitrate reduction.

## Materials and methods

### Site description and sampling

Plug flow-through reactors (FTRs) were used to determine rates of nitrate reduction, carbon mineralization and dissolved organic carbon (DOC) release in intertidal freshwater sediments from the upper estuary of the Scheldt River near Appels, Belgium. The site was chosen because of its high potential nitrate reduction rates (Laverman et al. 2006) and its large sedimentary organic carbon load (Wollast 1988). The biogeochemistry has been thoroughly characterized in a number of previous studies (Hyacinthe and Van Cappellen 2004; Laverman et al. 2006, 2007; Lin et al. 2007; Pallud and Van Cappellen 2006; Pallud et al. 2007). Benthic nitrate reduction at the site has been shown to be primarily due to denitrification to $N_2$ (Laverman et al. 2006).

Sediments were retrieved in August 2003 from the lower, un-vegetated mudflat, which is inundated during each tidal cycle. A shuttle corer was used to collect eight intact sediment slices from two different depth intervals: five from the 0–1 cm interval, and three from the 4–5 cm interval (Laverman et al. 2006). One slice from each was used to determine the sediment organic carbon (SOC) content, while the remaining slices were placed into FTR cells, sealed in anaerobic bags and brought to a climate-controlled laboratory where the experiments were started the following day.

### Flow-through reactor experiments

The FTR experiments ran for over 2000 hours by pumping a known input solution through the reactor at a constant flow rate using a digitally controlled peristaltic pump. During the first 1600 hours, "amended" reactors received an input solution of de-ionized water containing 2.5 mM potassium nitrate; "unamended" reactors received an input

solution of de-ionized water with no electron acceptor. Beyond 1600 hours, one of the amended and one of the unamended 0–1 cm reactors were also supplied with acetate (Table 1). The input solutions were continuously sparged with argon to insure dissolved oxygen could not enter the sediment reactors and a 0.2 μm filter at the exit of each reactor prevented entrainment of particulate matter with the outflow solution. A full description of the FTR design and operation can be found elsewhere (Pallud et al. 2007; Roychoudhury et al. 1998).

Sampling was carried out at various time intervals ranging from every 4–8 h at the beginning of the experiment, to every 20–120 h toward the end. For each sample, about 12 mL of outflow was collected in a Greiner tube and refrigerated until analysis. Three milliliter samples were also periodically collected into 10 mL gastight, He-purged septum vials for dissolved inorganic carbon (DIC) and methane analysis. To avoid atmospheric contamination, these samples were collected by inserting a hypodermic needle attached to the outflow tubing into the butyl rubber stopper of the septum vial.

Rates of nitrate consumption, DIC release, dissolved organic carbon (DOC) release and the production or consumption of any other analyte were determined for each sample using,

$$R = \frac{(C_{\text{out}} - C_{\text{in}}) \times Q}{V_{\text{sed}}} \quad (1)$$

where $C_{\text{in}}$ is the measured concentration in the input solution, $C_{\text{out}}$ is the measured concentration in the outflow, $Q$ is the measured flow rate and $V_{\text{sed}}$ is the sediment volume in the FTR (13.85 $cm^3$). Flow rate was measured for each sample by weighing them shortly after collection and deriving the volume discharged during the sampling period. On average the flow rate was about 3 mL $h^{-1}$ and varied by about 10% in each reactor over the course of the experiment. Variations in the flow rate between 1 and 12 mL $h^{-1}$ have been shown to have a negligible effect on metabolic rates measured with FTRs (Pallud et al. 2007).

### Analytical methods

Outflow solutions were analyzed for nutrients ($NO_3^-$, $NO_2^-$, $PO_4^{3-}$, $NH_4^+$), DIC, DOC, cations ($Ca^{2+}$, $Na^+$, $K^+$, and $Mg^{2+}$), total dissolved Fe and alkalinity. Nutrients were quantified by standard segmented flow colorimetric analysis on a Bran & Leubbe Autoanalyzer III. DOC was measured using a TOC Analyzer (Shimadzu TOC-50550A), cations were measured on an ICP-OES (Perkin Elmer Optima 3000), and alkalinity was determined by Gran titration. Total dissolved Fe measurements were made with the method detailed in Hyacinthe and Van Cappellen (2004). DIC was measured by acidifying the septum vial samples with phosphoric acid and quantifying the generated $CO_2$ on a TraceGC with thermal conductivity detector.

A limited number of methane determinations were carried out on a subset of samples using a TraceGC with flame ionization detector. Corrections were made to account for dissolved $CO_2$ and dissolved $CH_4$ in each vial based on the respective Henry's law coefficients and the measured pressure and temperature of each sample. Short chain fatty acids were analyzed on a limited number of samples by ion chromatography using a Dionex DX120 with an IonPac ICE-AS6 column and Anion-ICE Micro Membrane II suppressor.

## Results

### Nitrate reduction

Rates of nitrate reduction were measured in the 0–1 and 4–5 cm reactors for over 1600 hours (Fig. 1a). Initial

**Table 1** Experimental design for the carbon burnout and acetate addition phases of the long-term reactor experiments

| Reactor type | Sediment depth interval (cm) | Sedimentary organic carbon (wt%) | Input solution burnout phase (0–1600 hours) | Input solution acetate phase (1600–2200 hours) |
|---|---|---|---|---|
| Amended | 0–1 | 3.9 | 2.5 mM nitrate in anoxic water | 2.5 mM nitrate + 0.75, 1.5, 3.0, or 4.5 mM acetate in anoxic water |
| | 4–5 | 1.2 | | |
| Unamended | 0–1 | 3.2 | Anoxic water | 0.75, 1.5, 3.0, or 4.5 mM acetate in anoxic water |
| | 4–5 | 2.2 | | |

Note that the 0–1 cm reactors were run in duplicate

rates were in the range 100–150 nmol $cm^{-3}$ $h^{-1}$ in the 0–1 cm reactors and increased slightly within the first few days. Rates then began to decrease to around 40 nmol $cm^{-3}$ $h^{-1}$ by 400 hours. After this time, rates decreased more gradually reaching values near the detection limit (5 nmol $cm^{-3}$ $h^{-1}$) by about 1300 hours. Initial rates in the 4–5 cm reactor were lower compared to the 0–1 cm, but increased more strongly to 190 nmol $cm^{-3}$ $h^{-1}$ within the first few days. This initial increase was associated with a distinct build-up of nitrite in the reactor outflow (data not shown). After this peak, the rates declined more rapidly than was observed in the 0–1 cm reactors, reaching values below detection after 500 hours (Fig. 1a).

Once nitrate reduction rates had reached detection limit, it was presumed that the nitrate amended reactors had reached "carbon burnout" (i.e., the organic carbon available to the denitrifiers had been exhausted). This was confirmed by the near-instantaneous response of nitrate reduction activity to a supply of sodium acetate in the inflow of one of the 0–1 cm amended reactors (Fig. 3a). Within less than 24 h after adding 1.5 and 3.0 mM sodium acetate, nitrate reduction rates increased from near detection limit to 180 and 320 nmol $cm^{-3}$ $h^{-1}$, respectively. These rates were comparable to or greater than the initial nitrate reduction rates measured in the reactor (Fig. 1a). A third addition of excess acetate (i.e., 4.5 mM) resulted in near complete consumption of nitrate in the reactor, further confirming that nitrate reducing activity was limited by the availability of organic carbon substrates.

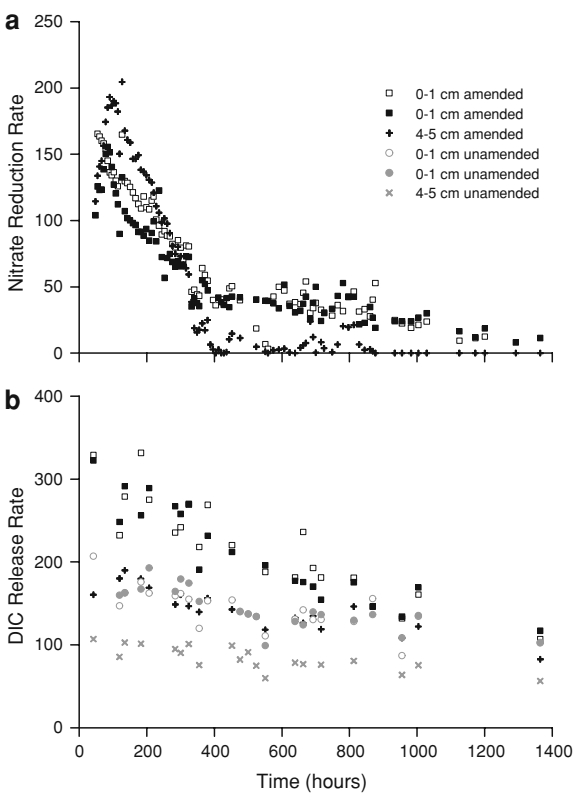


**Fig. 1** Nitrate reduction rates for amended reactors (**a**) and DIC release rates for amended and unamended reactors during the first 1400 hours of the experiment (**b**). All rates are in units of nmol $cm^{-3}$ $h^{-1}$. Rates observed at 1400 hours persisted until 1700 hours when acetate additions were made

## Dissolved inorganic and organic carbon release

Dissolved inorganic carbon release rates in the 0–1 cm amended reactors decreased in a roughly linear fashion from about 325 nmol $cm^{-3}$ $h^{-1}$ at the beginning of the experiment to about 120 nmol $cm^{-3}$ $h^{-1}$ by 1400 hours (Fig. 1b). In the deeper amended reactor, DIC release was initially on the order of 160 nmol $cm^{-3}$ $h^{-1}$ and increased slightly to 200 nmol $cm^{-3}$ $h^{-1}$ within the first several days. After this peak, however, the DIC release rate gradually decreased toward 90 nmol $cm^{-3}$ $h^{-1}$ by 1400 hours.

In the unamended reactors, DIC release was markedly lower in the beginning of the experiment compared to the amended reactors. Rates were initially around 200 nmol $cm^{-3}$ $h^{-1}$ in the 0–1 cm reactor and decreased gradually toward 120 nmol $cm^{-3}$ $h^{-1}$ by 600 hours. Rates then remained relatively stable until the end of the experiment. In the 4–5 cm reactor, rates decreased from initial values of 100 nmol $cm^{-3}$ $h^{-1}$ to about 60 nmol $cm^{-3}$ $h^{-1}$ by 1400 hours. Compared to the amended reactors, DIC release rates were initially lower in the unamended reactors, but the difference diminished over time until similar release rates were observed in both sets of reactors by 1400 hours.

Dissolved organic carbon release rates generally decreased in the first 500 hours of the experiment and remained relatively constant thereafter (Fig. 2b). Rates decreased from 110 to 5 nmol $cm^{-3}$ $h^{-1}$ within the first 500 hours for the unamended 0–1 cm reactors, and from 30 to 5 nmol $cm^{-3}$ $h^{-1}$ within the same time period for the unamended 4–5 cm

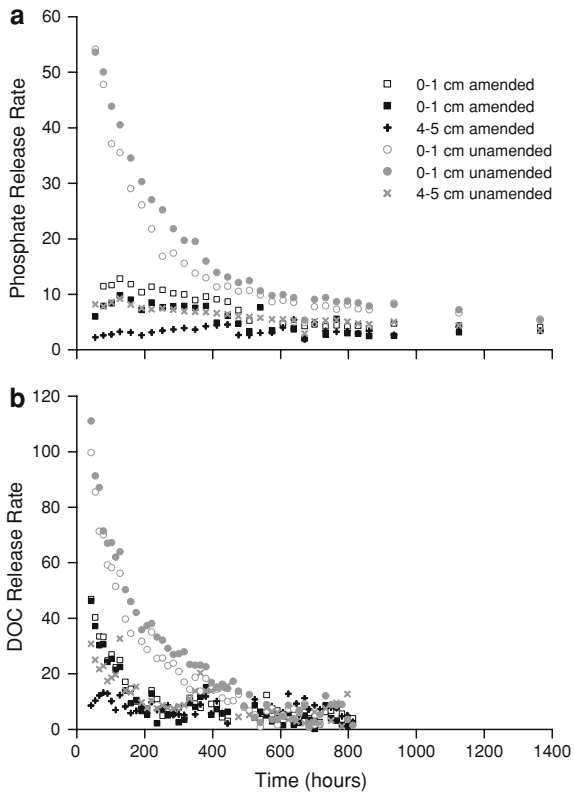


**Fig. 2** Phosphate release (**a**) and DOC release (**b**) rates for amended and unamended reactors during the first 1400 hours of the experiment. All rates are in units of nmol $cm^{-3}$ $h^{-1}$. DOC was not measured after 800 hours because concentrations had approached the instrument's detection limit

reactor. DOC release rates were roughly 50–90% lower than corresponding DIC release rates. The addition of nitrate to the amended reactors resulted in lower DOC release rates compared to the unamended reactors. Rates decreased from 50 to 10 nmol $cm^{-3}$ $h^{-1}$ by 300 hours for the amended 0–1 cm reactor, and varied in a narrow range from 0–10 nmol $cm^{-3}$ $h^{-1}$ for the entire experiment in the deeper amended reactor. After 500 hours, DOC release was similar for all reactors and no further DOC measurements were performed after 800 hours.

A fraction of the DOC release consisted of low molecular weight organic acids, in particular succinate and citrate, both of which were observed in the reactor outflow solutions during the first 800 hours of the experiments (data not shown). Succinate was the dominant organic acid identified, accounting for 5–15% of the DOC release in the unamended reactors.

## Phosphate release

Phosphate release rates in the unamended reactors decreased from 58 nmol $cm^{-3}$ $h^{-1}$ at the beginning of the experiment to around 5 nmol $cm^{-3}$ $h^{-1}$ by 1600 hours (Fig. 2a). Rates in the amended reactors were lower, declining from 10 nmol $cm^{-3}$ $h^{-1}$ at the beginning of the experiment to about 5 nmol $cm^{-3}$ $h^{-1}$ by 600 hours. Rates remained at this level in the amended cores for the remainder of the carbon burnout phase. After the carbon burnout phase, however, the acetate supply to one of the 0–1 cm amended reactors markedly altered the phosphate release rates. Rates rose to 8, 12 and 30 nmol $cm^{-3}$ $h^{-1}$ in response to successive additions of 1.5, 3.0 and 4.5 mM acetate (Fig. 3a). Additionally, when the input solution was switched back to a lower acetate concentration of 0.75 mM, a reduction in the phosphate release rate was observed.

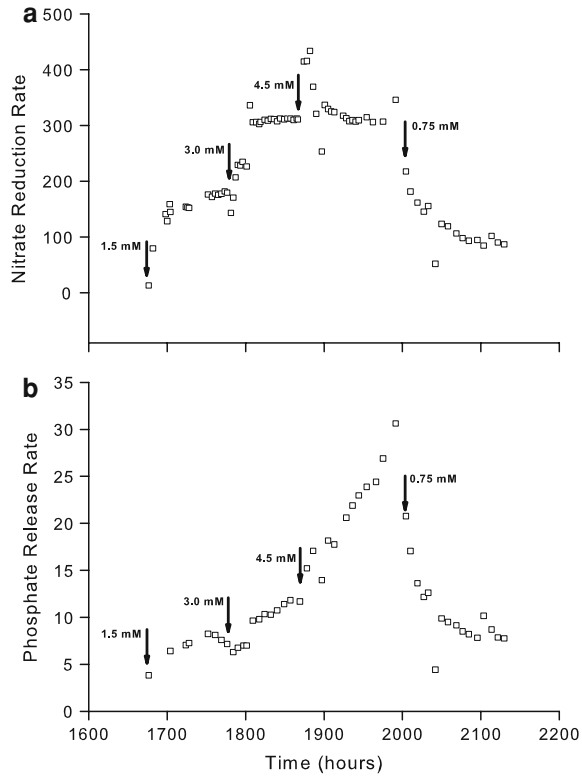


**Fig. 3** Nitrate reduction (**a**) and phosphate release (**b**) rates for one of the 0–1 cm amended reactors between 1600 and 2200 hours. All rates are in nmol $cm^{-3}$ $h^{-1}$. Sodium acetate was added at the times and concentrations indicated by the *arrows*

### Methane release

Due to technical reasons, headspace methane concentrations were only measured in a subset of samples taken after the carbon burnout and acetate addition phases of the experiments. During this period, methane production never exceeded the detection limit of 1 nmol $cm^{-3}$ $h^{-1}$ in any of the amended cores nor in the 4–5 cm unamended core. In the 0–1 cm unamended reactors, there was detectable methane production ranging from 3 to 19 nmol $cm^{-3}$ $h^{-1}$ with an average release rate of 8 nmol $cm^{-3}$ $h^{-1}$.

## Discussion

### Nitrate reduction rates

Rates of nitrate reduction measured during the first 150 hours (100–200 nmol $cm^{-3}$ $h^{-1}$, Fig. 1a) fall within the previously reported range of nitrate reduction rates for the upper centimeters of sediment at the Appels site (100–500 nmol $cm^{-3}$ $h^{-1}$, Laverman et al. 2006). The pronounced initial increase in nitrate reduction rate for the 4–5 cm reactor most likely reflects the growth of denitrifiers and the induction of nitrite reductase. The latter is consistent with the observed release of nitrite from the 4–5 cm reactor during the first 200 hours. Note that, because of the high in situ rates of denitrification at the site, nitrate is depleted within the upper millimeters of the sediment (Laverman et al. 2007). The 4–5 cm sediment is thus located well below the zone of in situ nitrate reduction.

The rate of nitrate reduction eventually drops to negligible values after about 1600 hours for the 0–1 cm reactors and 500 hours for the 4–5 cm (Fig. 1a). The decrease in nitrate reduction activity is attributed to the progressive depletion of bioavailable sedimentary organic carbon. As expected, the latter is depleted faster in the sediment from the deeper depth interval, which has been exposed for a longer time to both oxic and anoxic degradation (Hartnett et al. 1998; Hedges and Keil 1995). Limitation by bioavailable organic carbon is confirmed by the instantaneous reactivation of nitrate reduction activity when supplying acetate to one of the amended 0–1 cm reactors at the end of the carbon burnout phase. This result indicates that a viable population of nitrate reducers is present even after nitrate reducing activity has ceased. It further implies that the activity of nitrate reducers is not limited by the availability of the electron acceptor. Therefore, the sedimentary organic matter available for the denitrifying community seems to be completely utilized after about 1600 hours, or 2 months, of continuous nitrate supply.

### DIC release by $CaCO_3$ dissolution, iron reduction and methanogenesis

In order to derive the organic carbon mineralization rates due to nitrate reduction and fermentation, the measured DIC release rates in the amended and unamended reactors are corrected for DIC contributions from other biogeochemical processes. The processes considered include carbonate mineral dissolution, microbial iron reduction and methanogenesis.

Because sulfate is not supplied to the reactors, sulfate reduction is not considered as a potential source of DIC. In principle, oxidation of Fe(II) sulfide phases by nitrate could produce sulfate to support sulfate reducing activity in the amended reactors (Wieder and Lang 1988; Vile et al. 2003; Keller and Bridgham 2007). The resulting DIC release would ultimately be coupled to nitrate reduction, however. In addition, it has been shown that Appels sediments contain little iron sulfides, as solid-phase reactive iron is primarily bound to phosphate (Hyacinthe and Van Cappellen, 2004).

Sediments of the Scheldt estuary are enriched in calcium carbonate (Du Laing et al. 2007). Thus, inflow of undersaturated solutions may induce dissolution of $CaCO_3$ in the reactors. In principle, the amount of carbonate generated by $CaCO_3$ dissolution can be estimated from the flux of dissolved $Ca^{2+}$ exiting the reactor. A continuous release of dissolved $Ca^{2+}$ is indeed observed over the entire course of the experiments for both the amended and unamended reactors (Table 2). Initially, however, a fraction of the dissolved $Ca^{2+}$ is released from exchange sites of the sediment, a process that does not produce DIC. This is evident in the potassium nitrate amended reactors, where the retention of $K^+$ ions in the sediment is compensated by the release of exchangeable cations (Fig. 4). The near-unity slope of the linear trend in Fig. 4 implies that ion exchange with $K^+$ can account for the release of dissolved $Ca^{2+}$ in excess of the positive intercept along the *x*-axis.

**Table 2** DIC release rates in nmol $cm^{-3}$ $h^{-1}$ for the amended (*A*) and unamended (*U*) reactors at a number of selected times during the carbon burnout phase of the experiment

| Time (h) | Total DIC release rate[a] | | $CaCO_3$ dissolution[b] | | Iron reduction[c] | | Fermentation[d] | Nitrate reduction[e] |
|---|---|---|---|---|---|---|---|---|
| | *A* | *U* | *A* | *U* | *A* | *U* | *U* | *A* |
| 43 | 326 | 207 | 60 | 112 | 3 | 19 | 75 | 188 |
| 135 | 285 | 163 | 60 | 81 | 4 | 12 | 70 | 152 |
| 284 | 251 | 162 | 60 | 67 | 3 | 7 | 88 | 100 |
| 452 | 216 | 154 | 60 | 68 | 3 | 4 | 82 | 71 |
| 639 | 179 | 129 | 60 | 61 | 1 | 3 | 66 | 52 |
| 813 | 178 | 129 | 60 | 58 | 1 | 3 | 68 | 49 |
| 1004 | 165 | 135 | 60 | 56 | 1 | 3 | 76 | 28 |
| 1364 | 112 | 102 | 52 | 49 | 1 | 2 | 52 | 7 |
| 1600 | 126 | 116 | 50 | 50 | 1 | 2 | 64 | 11 |
| Integrated[f] | 4178 | 3034 | 1319 | 1378 | 45 | 96 | 1560 | 1198 |

[a] Total DIC release derived from measured DIC in outflow

[b] Contribution to DIC release derived from measured $Ca^{2+}$ in outflow

[c] Contribution to DIC release as derived from measured $PO_4^{3-}$ in outflow

[d] Difference between total DIC release and sum of $CaCO_3$ dissolution and iron reduction

[e] Difference between total DIC release and sum of $CaCO_3$ dissolution, iron reduction and fermentation

[f] DIC release in μmol integrated from 0 to 1600 hours

Once ion exchange reaches equilibrium any further $Ca^{2+}$ release can be ascribed to $CaCO_3$ dissolution. The corresponding rate is then subtracted from the DIC release to correct for carbonate released during $CaCO_3$ dissolution. As an example, for the reactor whose results are illustrated in Fig. 4, the non-zero intercept along the *x*-axis corresponds to a $CaCO_3$ dissolution rate of 60 nmol $cm^{-3}$ $h^{-1}$ (±10 nmol $cm^{-3}$ $h^{-1}$). In the unamended reactors, desorption of $Ca^{2+}$ from exchange sites is not significant because the inflow does not supply $K^+$ ions. Nonetheless, the release of dissolved $Ca^{2+}$ converges to nearly the same value after about 500 hours (56 ± 7 nmol $cm^{-3}$ $h^{-1}$), implying that within error, the $CaCO_3$ dissolution rates are the same in the amended and unamended reactor experiments (Table 2). Integrated over the carbon burnout phase, the contribution of carbonate dissolution is far from negligible, accounting for 32% of the total DIC production in the 0–1 cm amended reactors and 45% in the 0–1 cm unamended.

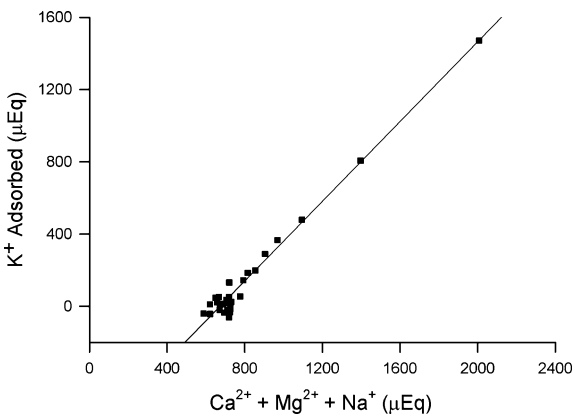


**Fig. 4** Charge balance between $K^+$ adsorbed and non-$K^+$ cations released from one of the 0–1 cm amended reactors. All units are in micro-equivalents (μEq). The ordinate was determined by summing $Ca^{2+}$, $Mg^{2+}$ and $Na^+$ concentrations in the reactor output and converting to charge equivalents. The abscissa was determined by subtracting the output $K^+$ concentration from the input. The linear regression through the data has a slope of 1.10, an *x*-intercept of 672 μEq and an $r^2$ of 0.98

The sediments at Appels also contain appreciable amounts of chemically and biologically reactive ferric iron, mainly in the form of hydrous ferric phosphate (Hyacinthe and Van Cappellen 2004; Lin et al. 2007). Reduction of this material will generate DIC and release dissolved phosphate and $Fe^{2+}$. Based on the inferred composition of the ferric iron substrate at the Appels site (Hyacinthe and Van Cappellen 2004), the following stoichiometry is assumed:

$$(Fe)_4(PO_4)_3(OH)_3 + CH_2O + 5H^+ \rightarrow 4Fe^{2+} + 3H_2PO_4^- + CO_2 + 2H_2O \quad (2)$$

Because $Fe^{2+}$ is highly particle-active, its concentration in the outflow solutions remains at or below the detection limit during the entire course of the experiment. Therefore the concentration of phosphate in the outflow is used to estimate the DIC release due to microbial iron reduction.

Qualitatively, the significantly lower release of phosphate from the amended reactors (Fig. 3a) agrees with the energetically more favorable reduction of nitrate compared to that of solid-phase ferric iron. In other words, the preferential utilization of nitrate over ferric iron is expected when nitrate is available in excess (Froelich et al. 1979; Zehnder and Stumm 1988). This inhibition is also illustrated by the response to the acetate additions at the end of the carbon burnout phase (Fig. 3b). When acetate is added in excess (i.e., the 4.5 mM acetate inflow), the nitrate supply becomes limiting and the excess acetate is then available to iron reducers. This results in a concomitant increase in the phosphate release rate. When the acetate addition is subsequently reduced to 0.75 mM, and nitrate thus becomes available again in excess, microbial iron reduction is inhibited and phosphate release decreases. Thus, we assume that phosphate release in the Appels sediments primarily reflects the dissolution of the hydrous ferric phosphate as it is utilized by microbial iron reduction.

Based on the measured phosphate release rates and assuming a molar DIC:$PO_4^{3-}$ ratio of 1:3 (Eq. 2), microbial iron reduction can account for only 1% of the integrated DIC release in the amended reactors (Table 2). In the unamended reactors, the contribution integrated over the first 1600 hours of the experiments is slightly higher, on the order of 3%. This contribution does vary with time, however. For example, microbial iron reduction could supply up to 10% of the DIC release during the first 200 hours of the experiment in the unamended reactors (Table 2).

As some phosphate release also derives from organic phosphorus mineralization, the above estimates represent upper limits on the contribution of iron reduction to DIC release. Assuming a Redfield stoichiometry of 106:1 for the atomic C:P ratio of sedimentary organic matter, roughly 26 μmol of organic P could be released from the amended reactor within the first 1600 hours—or about 19% of the total integrated phosphate release of 136 μmol P during the same time period. For the unamended reactors, this fraction is on the order of 5%.

The available $CH_4$ measurements imply negligible DIC production by methanogenesis. This is expected for the amended reactors where the excess supply of an external electron acceptor (nitrate) likely inhibits methane production (Capone and Kiene 1988). However, even in the case of the unamended reactors, the observed methane release can only account for about 2% of the total DIC release. Admittedly, this estimate is based on methane concentrations measured after the carbon burnout phase, when rates of methanogenesis may be substantially lower than earlier on during the experiment. However, in more recent FTR experiments with the same Appels sediments, methane release rates during the first 400 hours were found to be similarly low ($6 \pm 3$ nmol $cm^{-3}$ $h^{-1}$; P. Bots, personal communication).

The anaerobic degradation of organic matter in the absence of external electron acceptors produces $CH_4$ and $CO_2$ as terminal products. Methanogenesis is therefore expected to be an important degradation process in organic-rich, freshwater sediments, such as the ones studied here (Middelburg et al. 1995; Van der Nat et al. 1998; Van der Nat and Middelburg 2000; Hellings et al. 2000). The low rates of $CH_4$ release from the unamended reactors are thus somewhat surprising. Possibly, the concentrations of fermentation products that fuel methanogenesis (e.g., alcohols, acetate, $H_2$) remain too low to sustain high rates of methane production because of their continuous removal with the reactor outflow and their consumption by the resident iron reducing microorganisms.

## Carbon mineralization rate: determination

After correcting the DIC release rates for the contributions of carbonate dissolution, iron reduction and methanogenesis, the organic carbon mineralization rates (CMRs) due to nitrate reduction and fermentation can be calculated (Fig. 5). The estimated CMRs are typically 60–70 nmol $cm^{-3}$ $h^{-1}$ less than the DIC release rates and follow similar trends with time. This is primarily because the correction term is dominated by the near-constant contribution of $CaCO_3$ dissolution. The CMR values

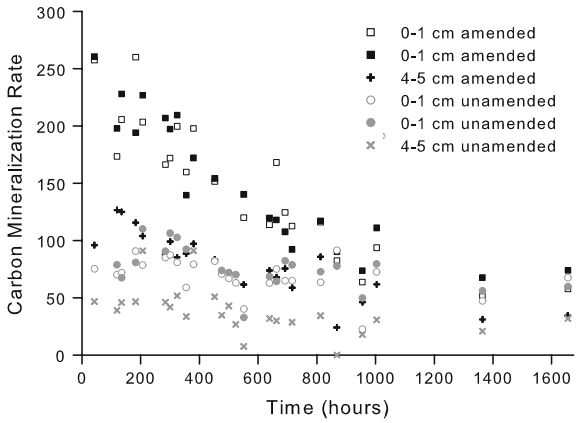


**Fig. 5** Carbon mineralization rates for amended and unamended reactors during the first 1700 hours of the experiment. All rates are in nmol $cm^{-3}$ $h^{-1}$. Rates were determined by subtracting the contributions of $CaCO_3$ dissolution and iron reduction from the DIC release rates in Fig. 1b

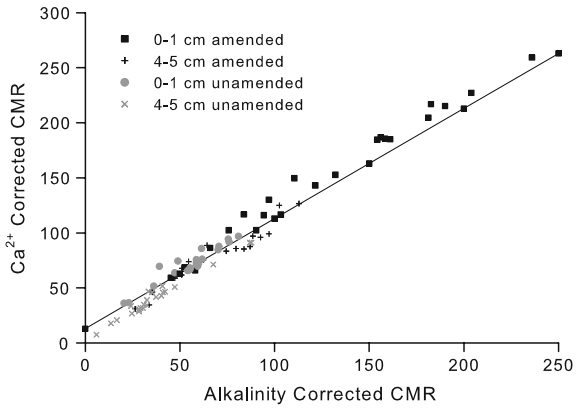


**Fig. 6** Comparison between $Ca^{2+}$-corrected and alkalinity corrected carbon mineralization rates for amended and unamended reactors. The *line* represents a 1:1 regression which has been drawn through an intercept of 11 nmol $cm^{-3}$ $h^{-1}$. This intercept reflects the excess CMR that is inferred by the $Ca^{2+}$ correction

are also quite sensitive to the magnitude of the $CaCO_3$ dissolution correction, especially during the final stages of the carbon burnout phase, between 1000 and 1600 hours. Hence, the CMR values are verified using an alternative method to correct the DIC release based on the measured alkalinities. The assumption inherent to this method is that the total alkalinity measured in the outflow reflects the sum of the alkalinities released by carbonate mineral dissolution, denitrification and dissimilatory iron reduction. The alkalinity production due to carbonate dissolution can then be obtained by subtracting the contributions of the other two processes from the measured total alkalinity.

The alkalinity contribution from nitrate reduction is derived from the measured nitrate reduction rate, assuming the following stoichiometry:

$$4NO_3^- + 5CH_2O + 4H^+ \rightarrow 2N_2 + 5CO_2 + 7H_2O \quad (3)$$

that is, for every mole of nitrate reduced, one equivalent of alkalinity is produced. The alkalinity contribution due to dissimilatory iron reduction is more complicated to determine. Based on Eq. 2, five equivalents of alkalinity would be generated per three moles of phosphate released. However, Eq. 2 assumes that all reduced iron is released to solution as $Fe^{2+}$. Dissolved iron, however, is not actually detected in any appreciable concentration in the outflow solutions. Most likely, $Fe^{2+}$ sorbs to sediment particles. If we assume that release of protons from sediment particles balances the charge of any adsorbed $Fe^{2+}$, then 8 protons would be required per mole of DIC produced in accordance with Eq. 2. As a result, a net reduction of one equivalent of alkalinity would accompany every mole of phosphate released.

The above approach yields alkalinity-derived CMR values that agree very well with those derived independently from the $Ca^{2+}$ release rate (Fig. 6). The small positive intercept for the $Ca^{2+}$-corrected CMRs suggests the $Ca^{2+}$-based correction may slightly underestimate the contribution of carbonate dissolution to DIC release. This would be expected if the dissolving carbonate mineral pool contains not only pure $CaCO_3$, but also magnesium and ferrous iron carbonates. This slight overestimation of the CMRs, however, does not affect the general conclusions of the study. In what follows, we keep using the CMRs derived from the $Ca^{2+}$-based correction (Fig. 5).

## Carbon mineralization rates: denitrification versus fermentation

Comparison of the CMRs between amended and unamended reactors implies that the availability and degradation kinetics of sedimentary organic matter are a function of the degradation pathway. Most notably, organic carbon degradation is significantly

faster and more extensive when nitrate is supplied (Fig. 5). Two possible reasons can explain the larger CMRs in the presence of nitrate: either fermentation is enhanced in the presence of nitrate resulting in an increased flow of fermentation by-products to the denitrifiers or, the denitrifiers are capable of accessing an additional pool of sedimentary organic matter that is not available to fermentors.

Stimulation of fermentation can occur when a terminal metabolic process consumes fermentation by-products, which otherwise build up in the pore water and inhibit further fermentation. Addition of an excess electron acceptor could thus result in lower by-product concentrations, thereby relaxing inhibition and causing fermentors to degrade more sedimentary organic carbon (SOC). Such stimulation has been reported for marine and freshwater sediment incubations (Beauchamp et al. 1989). In FTR experiments, however, the build-up of high by-product concentrations is counteracted by the continuous removal of dissolved reaction products with the outflow. As can be seen by comparing Figs. 2b and 5, beyond 400 hours the CMRs in the amended reactors remain significantly higher than in the unamended reactors, although the DOC concentrations are similar for the amended and unamended experiments. Hence, it is more likely the denitrifiers are able to access SOC that is not available to the fermenting community. This is not entirely unexpected, as denitrifiers are able to process a wide array of particulate organic compounds, similar to aerobic heterotrophic bacteria (Beauchamp et al. 1989).

The convergence of CMRs in amended and unamended reactors toward similar values in the late stages of the experiment ($\geq$1000 hours, Fig. 5) also supports the suggestion that fermentation rates are not affected by the presence of nitrate. If nitrate somehow stimulates fermentation, lower fermentation rates would have been expected in the amended reactors by the time nitrate reduction ceases. Instead, DIC production by fermentation at the end of the experiment seems independent of the extent of prior denitrification. By extension, we hypothesize that, for a given sediment depth interval, DIC production by fermentation is the same in the amended and unamended reactors throughout the experiment (that is, the presence or absence of nitrate does not affect fermentation processes). Based on this hypothesis, we can then estimate the contribution of denitrification to carbon mineralization by subtracting the CMRs measured in the amended reactors from that in the unamended. The new CMR values are referred to as "denitrifier CMR".

The internal consistency of the hypothesis is tested by comparing the rates of nitrate reduction to either denitrifier CMRs or total CMRs. (This comparison is only carried out for the 0–1 cm reactors as the 4–5 cm results are complicated by the inferred growth of denitrifiers and the induction of nitrite reductase during the initial phase of the experiment.) When the cumulative denitrifier CMR is plotted against cumulative nitrate reduction, a single slope of 1.5 is obtained (Fig. 7). This value is consistent with the molar $\Delta DIC/\Delta NO_3^-$ ratios expected for nitrate reduction coupled to the oxidation of a variety of organic molecules. For instance, most common alcohols, sugars, volatile fatty acids and amino acids yield ratios in the range 0.8–1.7, with a maximum value of 2.5 for the oxidation of formate. In contrast, when plotting the cumulative total CMR against nitrate reduction, the slope varies from 2 to 4 throughout the experiment (Fig. 7). These ratios are higher than can reasonably be expected for nitrate reduction coupled to sedimentary organic matter degradation. Thus, a reasonable relationship between carbon mineralization and nitrate reduction only emerges when the contribution of fermentation to

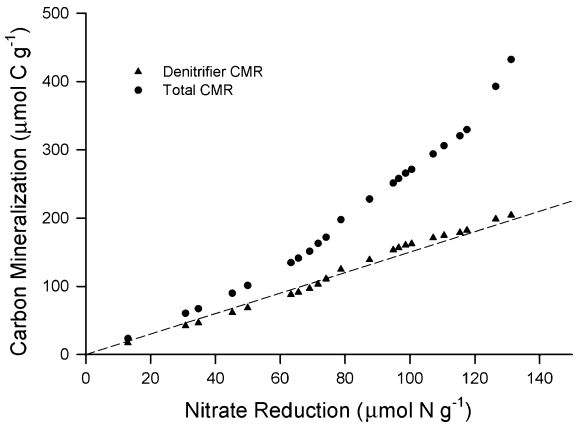


**Fig. 7** Comparison of cumulative carbon mineralization and cumulative nitrate reduction during the first 1600 hours of the experiment. Cumulative carbon mineralization was calculated by integrating either denitrifier CMR or total CMR. The slope of the regression line through the denitrifier CMR data was 1.5

DIC release in the amended reactors is explicitly accounted for.

The consistency of the corrected denitrifier CMRs supports the hypothesis that fermentation activity in the amended and unamended reactors is similar and, thus, independent of whether nitrate is supplied or not. A further implication is that a large fraction of the DIC production is due to fermentation processes, even when nitrate is supplied in non-limiting concentrations. In fact, integrated over the carbon burnout phase of the experiment, the amounts of organic carbon mineralized by denitrification and fermentation in the amended FTR experiments are of comparable magnitude (Table 2).

### Dissolved organic carbon release: unamended reactors

The DOC release observed in the unamended reactors (Fig. 2b) confirms the production of hydrolysis intermediates and fermentation by-products during the first 800 hours of the experiment. The presence of succinate and citrate also provides qualitative evidence that fermentation is taking place in these reactors. Quantitatively, however, the observed DOC release seems too low to explain the DIC release ascribed to fermentation. Integrated over the first 800 hours (the period for which DOC measurements are available), the total DOC release amounts to 402 μmol C, whereas DIC release ascribed to fermentation is 850 μmol C. The resulting 1:2 ratio of organic by-product to DIC release in the reactors is less than the typical 2:1 ratio expected for organic acid or alcohol fermentation (Das and Veziroglu 2001).

If fermentation is indeed responsible for the DIC release, there needs to be other reduced by-products formed that are not captured by the DOC analysis, such as $H_2$. Theoretically, if fermentation occurs via glycolysis in conjunction with the hexose monophosphate pathway, sugars can be fermented completely to $CO_2$ and $H_2$ (Das and Veziroglu 2001). This would result in an end-member 0:1 ratio of organic by-product to DIC release. Thus, a combination of mixed-acid, alcohol, and hydrogen fermentation could produce the ratios observed in the unamended reactors. Unfortunately, $H_2$ was not determined so there is no means of verifying this possibility for these experiments. However, the lack of terminal metabolic pathways that could generate significant DIC (namely iron reduction, sulfate reduction or methanogenesis) leads to the conclusion that the bulk of carbon mineralization occurring in the unamended reactors is due to fermentation.

### Dissolved organic carbon release: amended reactors

The supply of nitrate in the amended reactors significantly lowers the DOC release, compared to that of the unamended reactors, especially during the first 400 hours of the experiments (Fig. 2b). Qualitatively, this observation suggests that the denitrifiers utilize the organic by-products produced by fermentation. Quantitatively, however, the excess DOC supplied by fermentation is insufficient to account for the observed increase of CMR in the amended reactors. For example, when integrated over the carbon burnout phase of the experiment, the difference in DOC release between amended and unamended reactors is equivalent to 23 μmol C $g^{-1}$ dry sediment for the 0–1 cm reactor, and 2 μmol C $g^{-1}$ dry sediment for the 4–5 cm. These amounts represented only 12 and 4%, respectively, of the integrated carbon mineralization that is ascribed to denitrification in the 0–1 and 4–5 cm reactors.

Thus, the observed nitrate reduction rates in the amended reactors require a supplemental source of electron donors, presumably resulting from the hydrolysis of SOC not available to fermentation. This is in line with the results discussed in the previous section, which imply that the supply of nitrate results in additional carbon mineralization above that already being produced by fermentation. Possibly, fermentation may indirectly affect nitrate reducing activity in the reactors. The higher DOC release in the 0–1 cm sediment during the first 500 hours may stimulate the denitrifier community, thereby increasing their hydrolytic activity. Such stimulation of the oxidation of otherwise refractory organic matter by the addition of fresh DOC has been documented for sulfate reduction in anoxic marine sediments (Hee et al. 2001).

### Organic carbon bioavailability

In the nitrate-amended reactor experiments, denitrification, fermentation, dissimilatory iron reduction,

and methanogenesis together mineralize 10–13% of the total SOC by the time nitrate reduction becomes undetectable. This is true for both depth intervals. Denitrification and fermentation are each responsible for 40–50% of the total mineralization, with iron reduction and methanogenesis together contributing no more than 10%. When no nitrate is supplied to the reactor, only 3–9% of the SOC is mineralized over the course of the experiments. Thus, most organic matter in the upper centimeters of sediment at Appels is refractory, at least with respect to anaerobic decomposition, on the time scale of a few months. Periodic exposure to oxygen, which may occur during low tides when the sediment surface is exposed to air or during porewater irrigation by benthic macrofauna, may promote more extensive in situ organic carbon mineralization than observed here (Hartnett et al. 1998; Hedges et al. 1999). Further decomposition may also take place on much longer time scales than the ones considered here, but will have little effect on the benthic exchanges of DIC, DOC, electron acceptors and dissolved nutrient species.

In the amended reactors, a pronounced difference in organic carbon availability is observed with depth, with 4–5 times more organic carbon mineralized in the 0–1 cm reactor than in the 4–5 cm. In addition, the bioavailable organic matter is less reactive in the deeper sediment interval. This is illustrated by fitting the reactive continuum model of Boudreau and Ruddick (1991) to the time-dependent evolution of the available organic carbon utilized by the denitrifying community (Fig. 8). The continuum model assumes that the organic matter is made up of an infinite number of fractions with variable reactivity toward degradation. The initial available carbon concentrations and first-order degradation constants obtained from these fits are: 212 μmol C $g^{-1}$ dry sediment and 0.052 per day for the 0–1 cm reactor; 50 μmol C $g^{-1}$ and 0.037 per day for the 4–5 cm. Thus, a higher abundance together with a higher reactivity of bioavailable organic carbon explains the higher nitrate reduction rates in the shallow relative to the deeper sediment.

## Kinetics of denitrification

For any given time during the amended experiments, it is possible to calculate from the denitrifier CMR the concentration of available organic carbon still present in the reactors. In Fig. 9a, the rate of nitrate reduction measured in the 0–1 cm reactor is plotted against the available organic carbon concentration. Because the nitrate concentration is non-limiting during the experiment, this curve reflects the kinetic dependence of nitrate reduction on the bioavailable carbon concentration. The curve reveals two Michaelis–Menten type patterns with a rapid but relatively small increase in rate between 0 and 10 μmol C $g^{-1}$ dry sediment, a rate plateau between 10 and 80 μmol C $g^{-1}$ and a gradual but larger increase (possibly toward another rate plateau) at concentrations greater than 80 μmol C $g^{-1}$.

These patterns can be fit using a carbon degradation model that assumes a Michaelis–Menten dependency between nitrate reduction and denitrifier available carbon (Fig. 9a). A best fit to the data requires two reactive carbon pools: a lower reactivity pool which makes up 67% of the total available carbon, has a maximum rate of nitrate reduction ($R_{max}$) of 47 nmol $cm^{-3}$ $h^{-1}$, and a half-saturation constant ($K_m$) of 4.7 μmol C $g^{-1}$ dry sediment; and a higher reactivity pool which makes up the remaining 33% of the total available carbon, has an $R_{max}$ of 162 nmol $cm^{-3}$ $h^{-1}$, and a $K_m$ of 30 μmol C $g^{-1}$ dry sediment. Based on these results, the more reactive pool at Appels is able to sustain rates of denitrification that can be four times higher than the less reactive pool. However, the specific affinity (defined

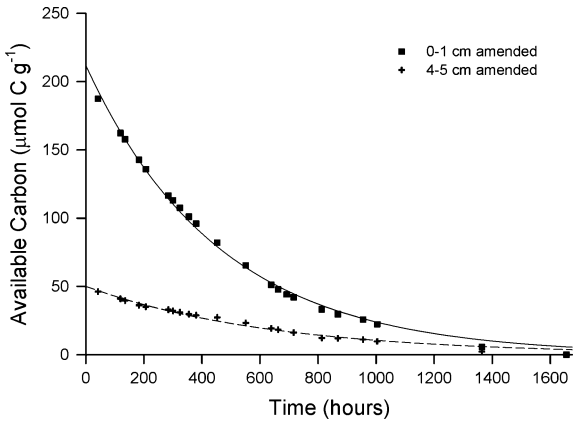


**Fig. 8** Denitrifier available carbon versus time in the 0–1 cm and 4–5 cm amended reactors. These data were determined from the difference in integrated CMR between amended and unamended reactors. *Lines* represent fits to the data using the reactive continuum model of Boudreau and Ruddick (1991)

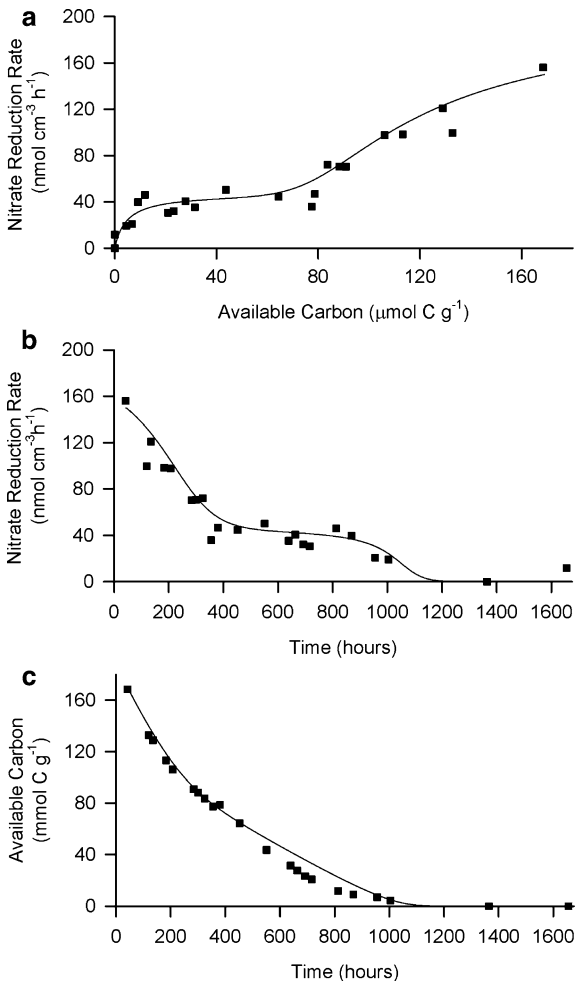


**Fig. 9** Nitrate reduction rate versus denitrifier available carbon concentration for one of the 0–1 cm amended reactors (**a**). Also shown are nitrate reduction rate versus time (**b**) and denitrifier available carbon concentration versus time (**c**) for the same reactor. Available carbon concentrations have been normalized to the dry sediment weight. *Lines* represent best-fits to the data using a two-component degradation model

as $R_{max}/K_m$) is twice as high for the less reactive pool. This implies that the denitrifying community is more efficient at processing the lower reactivity organic matter at Appels (Healey 1980). This may be a useful adaptation, as the less reactive particulate organic pool represents the larger fraction of reactive organic carbon in these sediments.

Using the same degradation model and kinetic parameters, it is also possible to reproduce the observed time-dependent evolution of the nitrate reduction rate (Fig. 9b) and the available organic carbon concentration (Fig. 9c). The difference in denitrifier CMR between the 0–1 and 4–5 cm depth intervals can then be explained by the higher abundance of the more reactive organic carbon pool in the 0–1 cm sediment. This pool is mainly oxidized during the first 400 hours, corresponding to the time span during which the denitrifier CMRs differs most between the two depth intervals (see Fig. 5). Afterwards, the CMR for both depth intervals converge toward similar, near-constant values between 400 and 800 hours. During the latter time span, the abundance of the less reactive pool remains well above its corresponding half-saturation constant, so the denitrifiers are processing the less reactive bioavailable organic matter at their maximum capacity. As a consequence, the concentration of available organic carbon decreases linearly with time until about 800 hours (Fig. 9c). Beyond 800 hours, the available organic carbon concentration becomes limiting and the rate of denitrification decreases to zero.

## Carbon budgets

Using the estimated CMRs and DOC release rates in conjunction with the estimated DIC production rates of iron reduction and methanogenesis, it is possible to construct carbon budgets for the FTR experiments (Fig. 10). These budgets integrate carbon fluxes over the first 1600 hours of the experiments, and assume that DOC release and carbon mineralization due to fermentation are similar in both amended and unamended reactors. When not directly determined from measurements, the integrated carbon fluxes are inferred from mass balance considerations. For example, the amount of DOC released by fermentation in the unamended reactor is estimated from the measured DOC release from the reactor, plus any DOC needed to support the carbon mineralization that is coupled to dissimilatory iron reduction and methanogenesis (Fig. 10b).

The most striking feature of the budgets is that fermentation is responsible for 50–75% of the combined DIC and DOC release from the reactors, whether or not nitrate is present (Fig. 10a, b). Even in the amended reactors, where nitrate concentrations are in excess, fermentation contributes more to DIC production than nitrate and iron reduction combined. This suggests that fermentation may be responsible for large fractions of the effluxes of DIC and DOC from sediments in the upper Scheldt estuary. Few

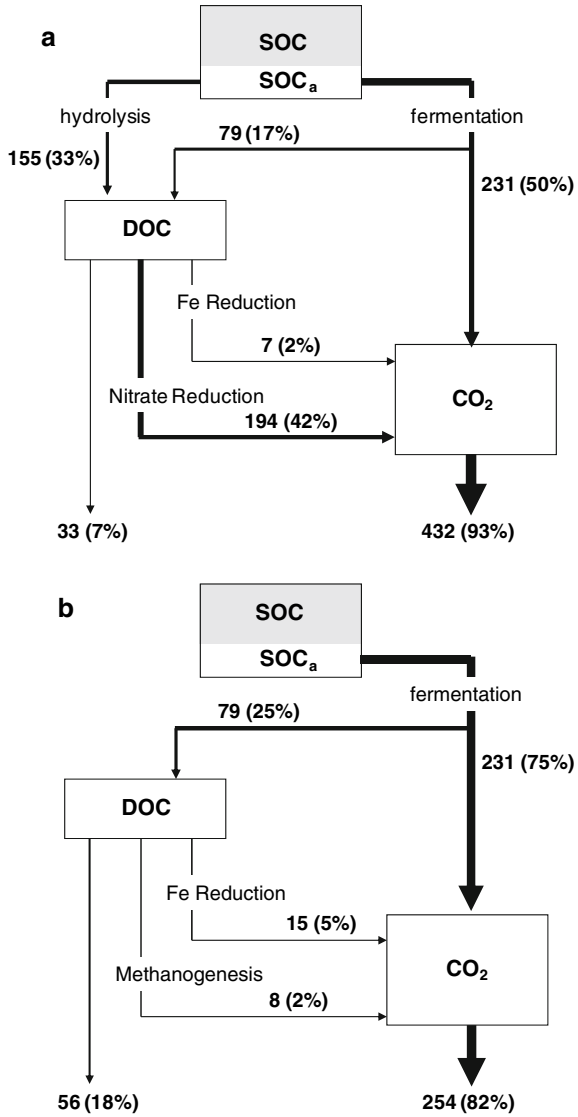


**Fig. 10** Carbon budget in μmol C $g^{-1}$ dry sediment for amended (**a**) and unamended (**b**) reactors during the first 1600 hours of the experiment. *Boxes* represent the carbon reservoirs: sedimentary organic carbon (SOC), available sedimentary organic carbon ($SOC_a$), dissolved organic carbon (DOC) and mineralized organic carbon ($CO_2$). *Arrows* represent the specific microbial degradation pathway: fermentation, iron reduction, methanogenesis, nitrate reduction, and the hydrolysis stimulated by the addition of nitrate. Any hydrolysis which precedes fermentation is implied. Values in parentheses represent the fractional contribution of each pathway to total carbon mineralization and solubilization

studies have investigated the contribution of fermentation to the production of DIC during the degradation of sedimentary organic matter. Our results, however, are consistent with the findings of Kerner (1993), who estimates that fermentation may account for up to one-third of the DIC production in the surface layer of an intertidal mudflat of the Elbe estuary. Furthermore, this author also finds that different respiration pathways and fermentation processes could co-occur in the sediment, as we document here.

Another striking feature of the data is that the supply of nitrate greatly enhances the degradation of organic matter in the sediments. An additional 155 μmol C $g^{-1}$ dry sediment is degraded when nitrate is supplied; this extra degradation accounts for 80% of the total organic carbon mineralized by denitrifiers (i.e., 155 out of 194 μmol $g^{-1}$ dry sediment). The other 20% of denitrifier carbon mineralization derives from the DOC released by fermentation, mainly during the first 400–500 hours of the experiment (see Fig. 2b). This DOC is made up of small organic acids and possibly alcohols which can be readily utilized by the nitrate reducers and thereby can contribute to the high nitrate reduction rates observed during the first 400 hours of the experiment.

## Conclusions

Only 3–13% of the total SOC present in the estuarine sediments is degradable over the 2 month time scale of the flow-through reactor experiments. Fermentation and nitrate reduction are the main pathways of SOC degradation in the experiments, with minor amounts mineralized by iron reduction and methanogenesis. Fermentation proceeds at comparable rates whether or not nitrate is supplied. The continued release of DIC after denitrification ceases further implies that fermentation utilizes organic substrates that are unavailable to nitrate reducers. Even when nitrate is supplied in non-limiting concentrations, fermentation is responsible for ~50% of the organic carbon mineralization. Fermentation may thus be a largely overlooked benthic source of DIC in estuarine and other nearshore environments characterized by high organic matter loadings.

Nitrate reduction is in part fueled by the production of DOC compounds by fermentation. However, most of the organic carbon mineralization coupled to nitrate reduction derives from the hydrolysis of SOC that is not utilized in the absence of nitrate. Thus, it appears that the fermentative and nitrate-reducing communities are largely relying on different pools of

SOC for their metabolism. These observations call into question the usual kinetic formulations used in models for the early diagenetic degradation of SOC, which are based on an initial, rate-limiting breakdown of particulate organic matter into smaller molecules that is common to all degradation pathways.

**Acknowledgments** The authors thank Pieter Kleingeld for invaluable assistance with experimental design and Dineke van de Meent, Helen de Waard and Pieter Bots for chemical analyses. This study was supported by the Netherlands Organisation for Scientific Research (NWO), through its Pioneer (PVC) and Veni Programmes (AML).

## References

Arnosti C (2004) Speed bumps and barricades in the carbon cycle: substrate structural effects on carbon cycling. Mar Chem 92:263–273. doi:10.1016/j.marchem.2004.06.030

Arnosti C, Holmer M (2003) Carbon cycling in a continental margin sediment: contrasts between organic matter characteristics and remineralization rates and pathways. Mar Chem 58:197–208

Beauchamp EG, Trevors JT, Paul JW (1989) Carbon sources for bacterial denitrification. Adv Soil Sci 10:113–142

Boudreau BP, Ruddick BR (1991) On a reactive continuum representation of organic matter diagenesis. Am J Sci 291: 507–538

Bruchert V, Arnosti C (2003) Anaerobic carbon transformation: experimental studies with flow-through cells. Mar Chem 80:171–183. doi:10.1016/S0304-4203(02)00119-6

Capone DG, Kiene RP (1988) Comparison of microbial dynamics in marine and freshwater sediments: contrasts in anaerobic carbon metabolism. Limnol Oceanogr 33:725–749

Das D, Veziroglu TN (2001) Hydrogen production by biological processes: a survey of literature. J Hydrogen Energy 26:13–28. doi:10.1016/S0360-3199(00)00058-6

Du Laing G, Vanthuyne DRJ, Vandecasteele B, Tack FMG, Verloo MG (2007) Influence of hydrological regime on pore water metal concentrations in a contaminated sediment-derived soil. Environ Pollut 147:615–625. doi: 10.1016/j.envpol.2006.10.004

Fenchel TM, Findlay BJ (1995) Ecology and evolution of anoxic worlds. Oxford University Press, Oxford

Froelich PN, Klinkhammer GP, Bender ML, Luedtke NA, Heath GR, Cullen D, Dauphin P (1979) Early oxidation of organic matter in pelagic sediments of the eastern equatorial Atlantic: suboxic diagenesis. Geochim Cosmochim Acta 43:1075–1090. doi:10.1016/0016-7037(79)90095-4

Hartnett HE, Keil RG, Hedges JI, Devol AH (1998) Influence of oxygen exposure time on organic carbon preservation in continental margin sediments. Nature 391:572–574. doi:10.1038/35351

Healey FP (1980) Slope of Monod equation as an indicator of advantage in nutrient competition. Microb Ecol 5:281–286. doi:10.1007/BF02020335

Hedges JI, Keil RG (1995) Sedimentary organic matter preservation and assessment: a speculative synthesis. Mar Chem 49:81–115. doi:10.1016/0304-4203(95)00008-F

Hedges JI, Hu FS, Devol AH, Hartnett HE, Tsamakis E, Keil RG (1999) Sedimentary organic matter preservation: a test for selective degradation under oxic conditions. Am J Sci 299:529–555. doi:10.2475/ajs.299.7-9.529

Hee CA, Pease TK, Alperin MJ, Martens CS (2001) Dissolved organic carbon production and consumption in anoxic marine sediments: a pulsed tracer experiment. Limnol Oceanogr 46:1908–1920

Hellings L, Van Den Driessche K, Baeyens W, Keppens E, Dehairs F (2000) Origin and fate of dissolved inorganic carbon in interstitial waters of two freshwater intertidal areas: a case study of the Scheldt Estuary, Belgium. Biogeochemistry 51:141–160. doi:10.1023/A:1006472213070

Hoppe HG (1991) Microbial extracellular enzyme activity: a new key parameter in aquatic ecology. In: Chrost RJ (ed) Microbial enzymes in aquatic environments. Springer, Berlin, pp 60–83

Hyacinthe C, Van Cappellen P (2004) An authigenic iron phosphate phase in estuarine sediments: composition, formation and chemical reactivity. Mar Chem 91:227–251. doi:10.1016/j.marchem.2004.04.006

Keller JK, Bridgham SD (2007) Pathways of anaerobic carbon cycling across an ombrotrophic-minerotrophic peatland gradient. Limnol Oceanogr 52:96–107

Kerner M (1993) Coupling of microbial fermentation and respiration processes in an intertidal mudflat of the Elbe estuary. Limnol Oceanogr 38:314–330

Laverman AM, Van Cappellen P, van Rotterdam-Los D, Pallud C, Abell J (2006) Potential rates and pathways of microbial nitrate reduction in coastal sediments. FEMS Microbiol Ecol 58:179–192. doi:10.1111/j.1574-6941.2006.00155.x

Laverman AM, Meile C, Wieringa EBA, Van Cappellen P (2007) Vertical distribution of denitrification in an estuarine sediment: integrating sediment flowthrough reactor experiments and microprofiling via reactive transport modeling. Appl Environ Microbiol 73:40–47. doi:10.1128/AEM.01442-06

Lehman RM, O'Connell SP (2002) Comparison of extracellular enzyme activities and community composition of attached and free-living bacteria in porous medium columns. Appl Environ Microbiol 68:1569–1575. doi:10.1128/AEM.68.4.1569-1575.2002

Lin B, Hyacinthe C, Bonneville S, Braster M, Van Cappellen P, Roling WFM (2007) Phylogenetic and physiological diversity of dissimilatory ferric iron reducers in sediments of the polluted Scheldt estuary, Northwest Europe. Environ Microbiol 9:1956–1968. doi:10.1111/j.1462-2920.2007.01312.x

Mayer LM (1989) Extracellular proteolytic enzyme activity in sediments of an intertidal mudflat. Limnol Oceanogr 34: 973–981

Middelburg JJ, Klaver G, Nieuwenhuize J, Vlug T (1995) Carbon and nitrogen cycling in intertidal sediments near Doel, Scheldt Estuary. Hydrobiologia 311:57–69. doi: 10.1007/BF00008571

Pallud C, Van Cappellen P (2006) Kinetics of microbial sulfate reduction in estuarine sediments. Geochim Cosmochim Acta 70:1148–1162. doi:10.1016/j.gca.2005.11.002

Pallud C, Meile C, Laverman AM, Abell J, Van Cappellen P (2007) The use of flow-through sediment reactors in biogeochemical kinetics: methodology and examples of applications. Mar Chem 106:256–271. doi:10.1016/j.marchem.2006.12.011

Roychoudhury A, Viollier E, Van Cappellen P (1998) A plug flow-through reactor for studying biogeochemical reactions in undisturbed aquatic sediments. Appl Geochem 13:269–280. doi:10.1016/S0883-2927(97)00064-4

Roychoudhury A, Van Cappellen P, Kostka JE, Viollier E (2003) Kinetics of microbially mediated reactions: dissimilatory sulphate reduction in saltmarsh sediments (Sapelo Island, Georgia, USA). Estuar Coast Shelf Sci 56:1001–1010. doi:10.1016/S0272-7714(02)00325-6

Van Cappellen P, Gaillard JF (1996) Biogeochemical dynamics in aquatic sediments. In: Lichtner PC, Steefel CI, Oelkers EH (eds) Reactive transport in porous media: general principles and application to geochemical processes. American Mineralogical Society, Washington, DC, pp 335–376

Van der Nat FJ, Middelburg JJ (2000) Methane emission from tidal freshwater sediments. Biogeochemistry 49:103–121. doi:10.1023/A:1006333225100

Van der Nat FJ, Middelburg JJ, Van Meteren D, Wielemakers A (1998) Diel methane emission patterns from *Scirpus lacustris* and *Phragmites australis*. Biogeochemistry 41: 1–22. doi:10.1023/A:1005933100905

Vile MA, Bridgham SD, Wieder RK (2003) Response of anaerobic carbon mineralization rates to sulfate amendments in a boreal peatland. Ecol Appl 13:720–734. doi:10.1890/1051-0761(2003)013[0720:ROACMR]2.0.CO;2

Wieder RK, Lang GE (1988) Cycling of inorganic and organic sulfur in peat from Big Run Bog, West Virginia. Biogeochemistry 5:221–242. doi:10.1007/BF02180229

Wollast R (1988) The Scheldt Estuary. In: Salomons W, Bayne BL, Duursma EK, Forstern U (eds) Pollution of the North Sea. An Assessment. Springer, Berlin, pp 183–192

Zehnder AJB, Stumm W (1988) Geochemistry and biogeochemistry of anaerobic habitats. In: Zehnder AJB (ed) Biology of anaerobic microorganisms. Wiley, New York, pp 1–38